14. *Experimental Investigation of the Deformation of Sand Mass. Part IV.*

By Naomi MIYABE,

Earthquake Research Institute.

(Received March 20, 1934.)

1. Introduction. In our previous papers[1], we described and discussed the results of experiments on the deformation of sand mass caused by receding and pressing one of the lateral walls, of the box enclosing the sand. In discussing the results of these experiments with reference to geophysical phenomena, it was considered desirable to carry out further experiments covering the case in which the sand mass rests on a layer of a very viscous liquid. In the present experiment, therefore, the sand mass rests on a layer of "Miduame", the Japanese rice jelly, the coefficient of viscosity, η, of which is of the order of 10^4-10^5 in c. g. s. unit, as will be shown later. It is probable that there are other substances suitable for use as the viscous substratum. The reason for our having selected "Miduame" for the purpose is that it is a substance of considerable viscosity, which can be obtained with ease. Its approximate density of 1·4, compared with 1·4 of the sand mass, piled up naturally, was another recommendation in its favour.

Owing to the great viscosity of the substratum used, the apparatus employed for the experiment had to be modified in several points, as will be described in the next paragraph.

2. Apparatus for the Experiment. The apparatus in the present experiment consists of two parts; that is, as in the case of the previous experiments, the vessel containing the sand mass and the layer of "Miduame" and the prime mover, or the pressing wall with reducing gear apparatus. The vessel frame was moulded of cast iron having the dimensions of 50 cm. × 20 cm. × 20 cm., its longer lateral sides being of glass plates of 1 cm. thickness. The thick glass plates are used because the lateral pressure acting on the glass plates, by the layers of sand and "Miduame", is so great as to smash the glass plates, if they were thin.

1) T. TERADA and N. MIYABE, *Bull. Earthq. Res. Inst.*, 4 (1928), 33; 6 (1929), 109; 7 (1929), 65.

The plan of the reducing gear apparatus is shown schematically in Fig. 1 and its photograph in Fig. 2.

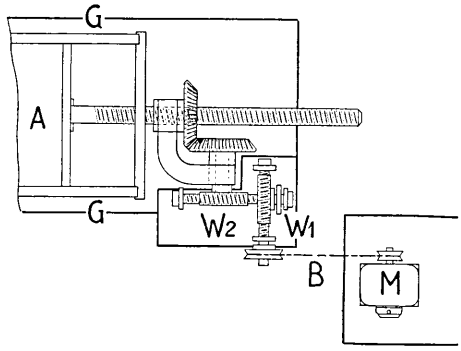

Fig. 1. Plan of the apparatus for driving the pressing wall.
G: Glass plates of 1 cm. in thickness.
A: Pressing wall.
W_1, W_2: Worm gears.
B: Belt. M: Motor.

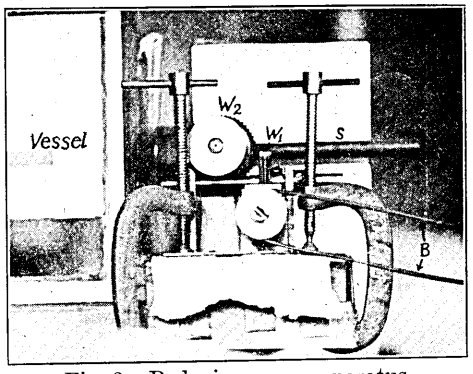

Fig. 2. Reducing gear apparatus.
W_1, W_2: Worm gears.
B: Belt.
S: Shaft of pressing Wall.

As shown in Figs. 1 and 2, the reducing gear consists of two sets of worm-gears, W_1 and W_2. The velocity of rotation of the motor, which is the power source for driving the pressing wall, is reduced by these gears to 1/10000, so that throughout the present experiments the velocity of the pressing wall A can be adjusted to 2/4−2/8 mm./min. Thus, by the use of the motor the fluctuation in velocity is reduced considerably in comparison with the previous experiments wherein the pressing wall was driven with a screw by hand. The speed of the pressing wall in the present experiment is much smaller than in the cases of the previous experiments, since greater speed will cause the collapse of the wall A, which is made of wood, owing to considerable stress that will be applied to the wall on account of the great viscosity of "Miduame", in which the wall is immersed.

It may be added that the pressing wall has the shape as shown in Fig. 3, so that "Miduame" in front and in the rear of the wall is communicating with each other through the clearance in the lower part of the pressing wall. If it were not for such clearance, the thickness of the layer of "Miduame" in front of the pressing wall would be increased by $khdl/l$, as the wall is moved forwards, where h is the depth, l the length of the layer of "Miduame", dl the amount of horizontal displacement of the wall and k constant. The constant k

is such that it becomes greater than unity when " Miduame " is deformed only where it is close by the pressing wall. Owing to the clearance in the lower part of the wall, and the sufficient slowness of the speed of the pressing wall, the effect of increase in the thickness of " Miduame " layer, which is required, can be disregarded.

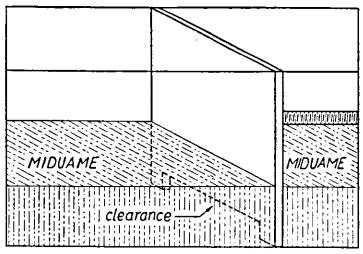

Fig. 3. Shape of the pressing wall.

3. Experiment. In beginning the experiment, 3 to 4 kg. of " Miduame " are first poured into the vessel to a depth of about five centimetres. Since many air bubbles, large and small, are held in " Miduame " thus poured out, it is allowed to stand for several days untill all visible signs of them have vanished. The sand is then carefully laid over " Miduame ", so that no movement of " Miduame " shall be caused by the inequality of loads on the different sides of the wall. On placing the sand mass over the layer of " Miduame ", a number of thin layers of white sand were interposed to serve as the reference marks. Thus prepared, the wall A, driven by the motor, is started to move forwards pressing against the sand mass. While the wall is moving forward, the successive forms of the deformed sand mass with white mark lines are photographed, at equal intervals of time from the longer lateral side with glass wall.

It is notable that even when the pressing wall is driven by motor, the velocity of the pressing wall is affected by fluctuations in rotation of the motor. The fluctuation, δv, in the velocity of the wall is related to the fluctuation in the rotation of the motor, δn, by the relation

$$\delta v/v = \delta n/n.$$

By assuming $n = 1000$ and $\delta n = 10$ per minute, the value of $\delta v/v$ will then be of the order of $1/100$. In practice the advancing velocity of the wall is very small, namely, 1/2 mm./min. for experiment Series IV and V, and 1/4 mm./min. for Series VI and VII. Provided it does not occur abruptly, the said effect of the fluctuation in velocity of the wall in these slow pressings may not seriously affect the mode of deformation. In Figs. 4 and 5, the amounts of displacement of wall A are plotted against the time measured on the photographs of Series V and VII.[2]

2) As it is assumed that the successive figures are photographed at equal time intervals, there will be errors in the time due to this assumption. But such errors may be smaller compared with those due to the rotational fluctuation of the motor.

In fact there are observed certain fluctuations in the velocity, but being very small, the velocity may practically be regarded as constant. We can therefore use the amounts of displacement of the pressing wall, x, instead of time, in plotting the quantities which vary in relation to the progress of the deformation.

The sand used for the present experiment was carefully washed, dried and sifted through 1 mm.^{2} and 1/4 mm.^{2} meshes. As, in the case of the present experiment, the layer of "Miduame" will be deformed considerably on pressing the sand mass to bring it to the state that may be called closely packed, the experiments were carried out only

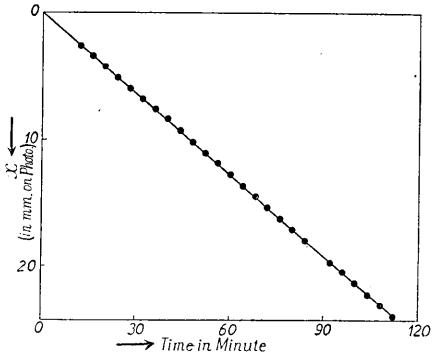

Fig. 4. Displacement of the pressing wall with regard to the time, for Series V.

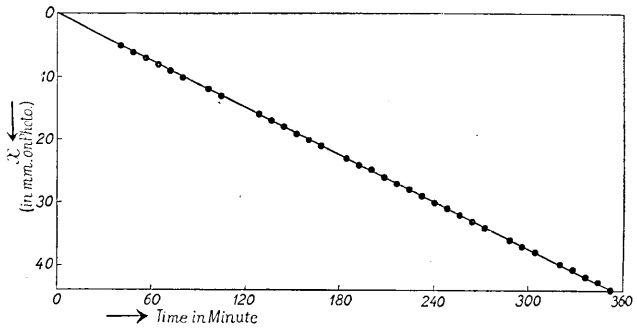

Fig. 5. Displacement of the pressing wall with regard to the time, for Series VII.

with loosely packed sand.[1]

It is well known that the porosity of the sand mass is an important factor determining its mechanical properties. It was, therefore, measured by the following simple method. The sand is first piled up in a meter-glass, its volume in bulk is thus measured to be V_1 cc., when V_2 cc. of water is added. The air filling the spaces between the sand grains is driven out and the net volumes of the sand and the water measured at the level of the water to V_3 cc. Then the porosity P of the original pile of the sand mass will be

$$P=[V_1-(V_3-V_2)]/V_1.$$

The porosity of the sand mass used in the present experiment was

thus measured to be 54·6 % on the average.

Certain physical properties of " Miduame " will also affect the mode of deformation of the sand mass, of which viscosity seems to be the most important. Its viscosity was measured by the " falling ball method ", at various room temperatures. The result of the measurement is shown in Fig. 6, in which the coefficient of viscosity, η, is plotted against the temperatures. As shown in Fig. 5, the coefficient of viscosity of " Miduame ", amounting to some 6×10^4 c. g. s. at 20°C decreases with increasing temperature following a certain curve. The room temperature at most times was 20°C, in most cases. It is also notable that a crust sometimes forms over the surface of " Miduame", due, on the one hand, to lower room temperature in winter, and, on the other hand, due to desiccation and also to the fine dust that deposits on the surface. When the sand mass is piled over the surface of " Miduame ", another sort of surface crust forms by permeation of " Miduame " several milimetres into the pore space of the sand mass. The surface crust thus formed is of considerable strength, and it can support the weight of lead balls several milimeters diameter. It may, therefore, affect in some measure the development of the slip planes in the sand mass when exposed to lateral compression. The mode of deformation of the sand mass in Series VII of the present experiement might have been affected by such a surface crust.

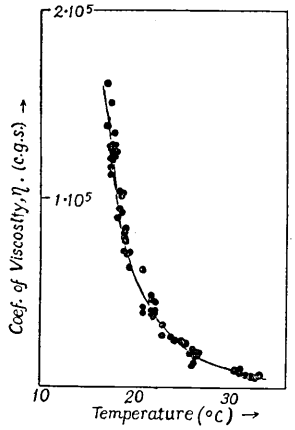

Fig. 6. Coefficient of viscosity of *Miduame* as a function of temperature.

4. The Results of the Experiments. The photographs of the successive forms of the sand mass deformed by lateral compression taken from the longer lateral side are shown in Plates, Figs. 7–57. The modes of deformation differs more or less for the different series of experiments. In this paragraph, only two of the series will be described, since, in their general modes of deformation, the other series are similar to either one or the other of these two. One of them, Series V, obtained when the sand mass is compressed by the wall with a velocity of 1/2 mm./min., and the other, Series VII, when the velocity of the wall is 1/4 mm./min. Comparing these two series of photographs, we notice a decided difference in the modes of deformation, as will be described later in greater detail. A difference, however, may not be entirely due to the difference in the velocity of the pressing wall, but probably to

the interference of the surface crust formed on the boundary surface of the sand and "Miduame", as mentioned in the preceding paragraph.

The mode of deformation of the sand mass of Series V will now be described in greater detail.

The initial stage of the deformation is not clear, but there appear systems of slip lines, or slip planes, *AC*, *BC*, *CD* and *CE*, as shown schematically in Fig. 58. These slip lines become clearly observable, when the deformation has proceeded to a certain extent, by the difference in the direction traced by the moving sand grains.

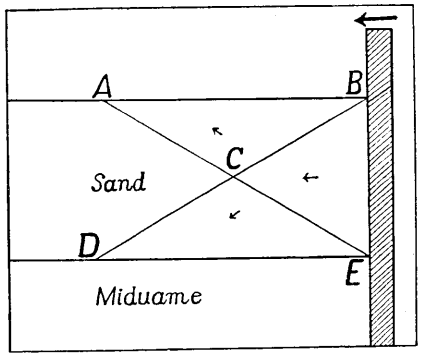

Fig. 58. Slip lines supposed to be developed initially in the sand mass.
(Large arrow denotes the direction of compression)
(Small arrows denotes the direction of grain motion)

As the pressing wall proceeds further, a wedge-shaped part of the sand mass close to the wall, *BCE* in Fig. 58, is pushed forth and one of the contiguous wedge-shaped parts, *ACB*, is pushed upward, while another wedge-shaped part, *ECD*, is pushed downward. The shape and size of the wedge-shaped parts *ACB* and *ECD* are generally not alike, that is, the former is generally larger than the latter, with the result that the horizontal line *CF* does not always coincide with, but lies generally lower than the median line. Such a configuration of the wedge-shaped parts is shown in Fig. 59, schematically. The inclinations of these slip lines, *AC*, *BC*, *DC* and *EC* are as a rule also different. The variation in inclination of these slip lines against the horizontal lines, θ, θ', φ, φ', together with the height of the line *CF* from the base, *H*, the lengths of *AB*, *CF*, *ED*, that is, *l*, *c*, *b*, are plotted against the amount of displacements of the wall, *x*, in Figs. 60 and 61, respectively.

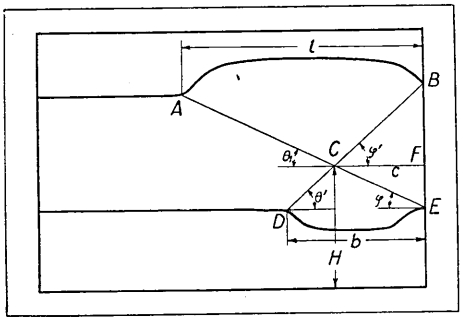

Fig. 59. Schematical figure showing the slip planes developed in the sand mass, for Series V.

In these curves showing variations in the factors of the successive figures of the deformed sand mass we notice; i) that the angles θ, θ', φ

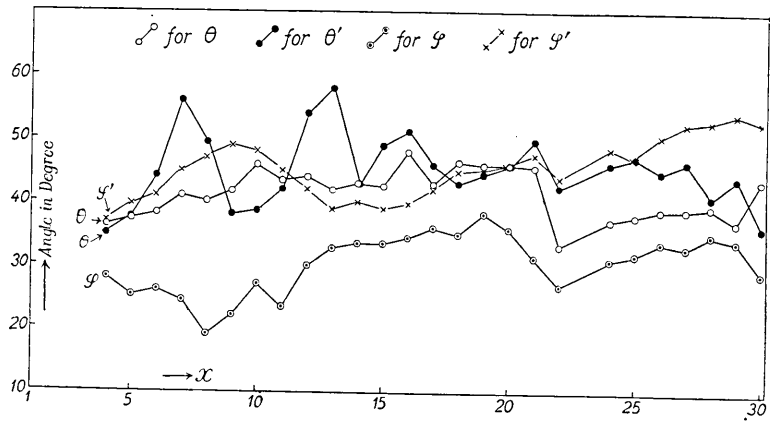

Fgi. 60. Variation of θ, θ', φ, φ' for Series V.

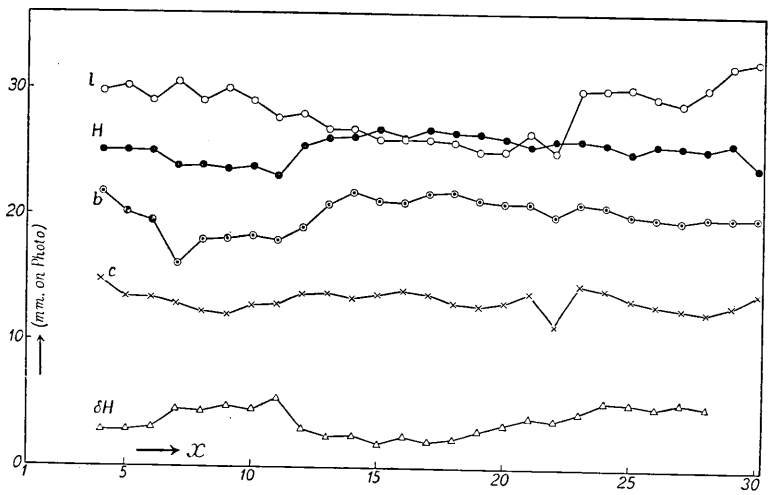

Fig. 61. Variation of l, b, c, H and δH for Series V.

and φ' tend to 30° (approximately) at the initial stage, that is, both $(\theta+\varphi')$ and $(\theta'+\varphi)$ are approximately 60°, which is in good accord with the value of $(\pi/2-\psi)$[3] as required by the theory of plastic deformation of the material, in which ψ, the angle of repose of the sand, is assumed as usual to be 30°; and ii) that there are comparatively acute changes in the values of φ, φ', b and H at $x=11$, as well as in the values of θ, θ', φ, φ' and l at $x=22$. These fairly acute changes in the values of θ, φ, etc., may, on the one hand, be due to errors of measurements, while on the other hand, it may also be due to certain changes in

3) Referred to p. 87 of the third report, *loc. cit.* 1)

physical conditions, in the interior of the sand mass, that has yielded to compression. In order to learn something of the changes in the physical conditions in the sand mass, changes were measured of the deformed areas, S of the sand mass on each sheet of the photographs by means of planimeter, as a measure of the deformed volume as shown in Fig. 62. The values indicating the deformed volume of the sand mass measured by this method may, however, contain considerable errors. Hence, though its variation with regard to x is to a certain extent

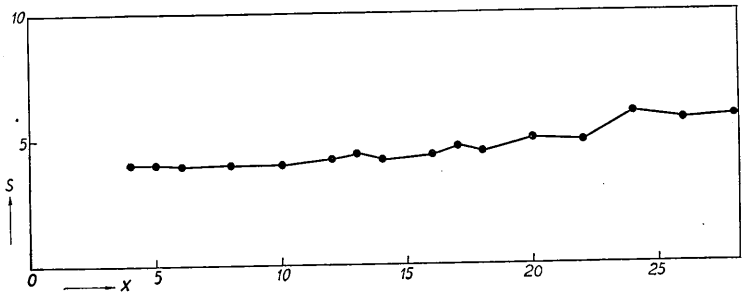

Fig. 62. Variation of S, for Series V.

parallel to the other factors, as shown in Fig. 62, any definite conclusion cannot be drawn for the present.

As to Series VII, the mode of deformation of the sand mass differs in several respects from that of Series V. In describing the mode of deformation observed in this series, it is convenient to distinguish three different stages of deformation. Schematical figures corresponding to the first and the third stages are shown in Fig. 63ab. In the first stage, the slip lines that developed in the deformed sand mass are ED, BD, CF and aA. The point A, the intersection of the slip lines BD

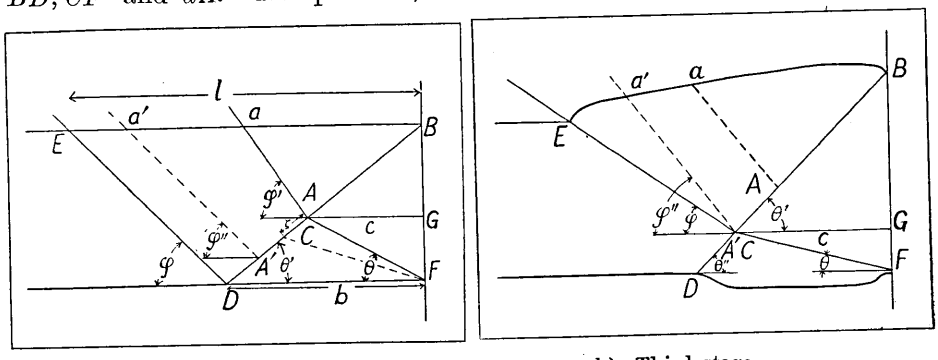

a) First stage. b) Third stage.

Fig. 63. Schematical figures of the mode of deformation of the sand mass for Series VII.

and aA, approximately agrees with point C. It will also be noticed that the traces of moving sand grains in part aAB are obviously longer than those in part $aADE$. After a while, however, when the pressing wall has travelled some sensible distance, another slip line, $a'A'$, is found to have developed within the region $aADE$. Corresponding to the end of the first stage, that is, the beginning of the second stage, we notice somewhat discontinuous changes at $x=22$ in the trends of the curves showing the variations of the factors θ, φ, etc. respectively,

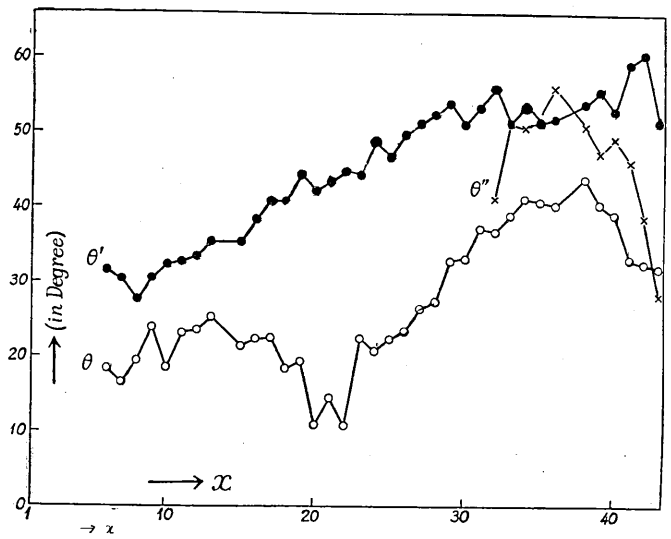

Fig. 64a. Variation of θ, θ' and θ'' for Series VII.

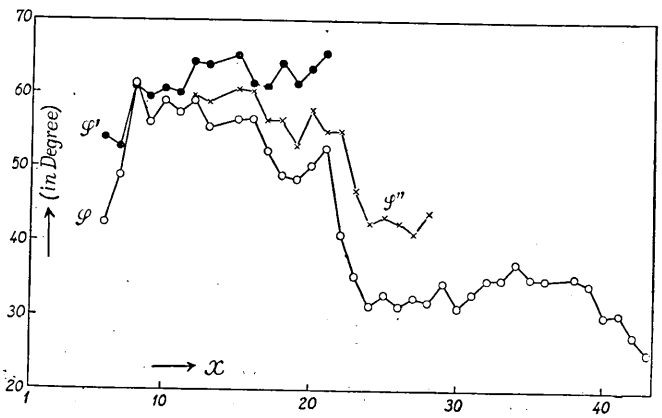

Fig. 64b. Variation of φ, φ' and φ'' for Series VII.

all of which are plotted, as before, against the displacements of the wall, x, as shown in Fig. 64ab.

Towards the end of this stage, the point C begin to move toward A' along the slip line $BAA'D$. The amount of departure of point C from point A, ζ, is plotted against x in Fig. 65. As may be seen in this figure, point C, which moves slowly at the beginning, moves rapidly towards the end, until it coincides with point A'. Then the second stage commences. Corresponding to the beginning of the third stage at $x=30$, we notice that the inclination, θ'', of CD, that is, a part of the

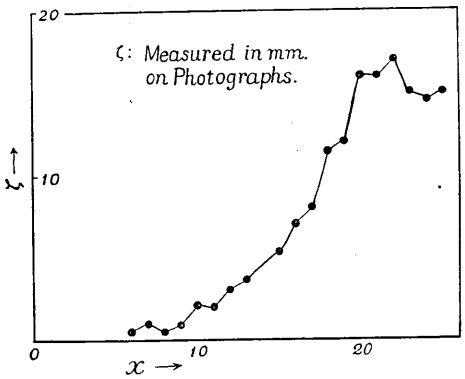

Fig. 65. Variation of ζ for Series VII.

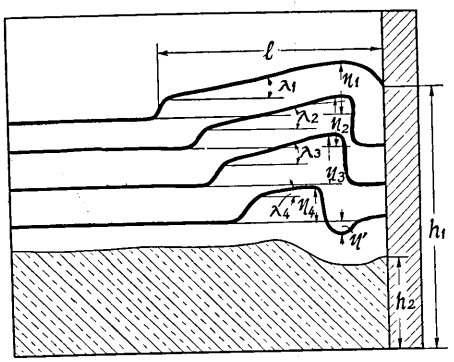

Fig. 66. Schematical figure of the mode of the deformation of the white marks in sand mass for Series VII.

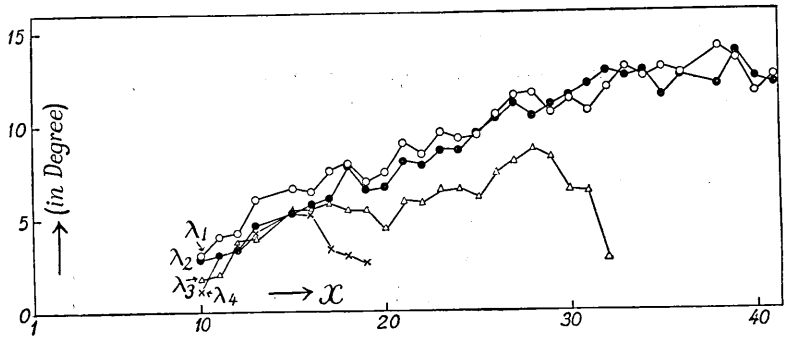

Fig. 67. Variation of λ_1, λ_2, λ_3 and λ_4 for Series VII.

slip line BD, begins to deviate from that of BC, θ', as shown in Fig. 64a, but we cannot notice abrupt changes in θ, φ, etc. Since in this stage,the slip lines aA and DE become insignificant, the mode of deformation becomes the same as those observed in the case of Series V.

Since as remarked above, the velocity of movement of the sand grains

in part EDB is greater in the region close to slip line ED than those in region aAB, the surface of part EDB of the sand mass and the segments of the lines of white sand in that part are tilted toward the direction of compression, as shown schematically in Fig. 66. The inclinations λ_1, λ_2, λ_3, λ_4 and the amounts of upward and downward displacements η_1, η_2, η_3, η_4, η_4' of the surface and the segments of the white lines may also be regarded as factors affecting the degree of deformation. They are plotted against x in Figs. 67 and 68. In these figures, we

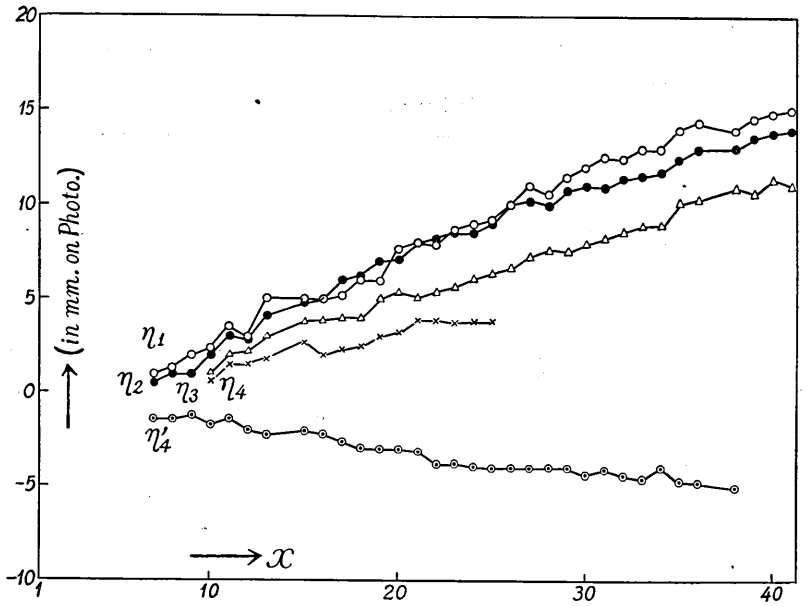

Fig. 68. Variation of η_1, η_2, η_3 and η_4' for Series VII.

notice again somewhat abrupt changes in the factors corresponding to the changes in stages, $x=22$ and $x=30$. The variations in λ's and η's may rather be regarded as corresponding to variations in physical conditions in the interior of the sand mass undergoing deformation. It is, therefore, probable that the curve showing the variation in λ's and η's may be related in some way with that indicating the variation in volume of the sand mass deformed. The actual volume of it, however, cannot be measured. Hence, as before, the lateral area of the deforming sand mass has been measured, as a provisional measure of its volume, on each sheet of the series of photographs. The result is shown plotted against x in Fig. 69. As has been remarked already in connection with S for Series V, errors included in the values of S being considerable,

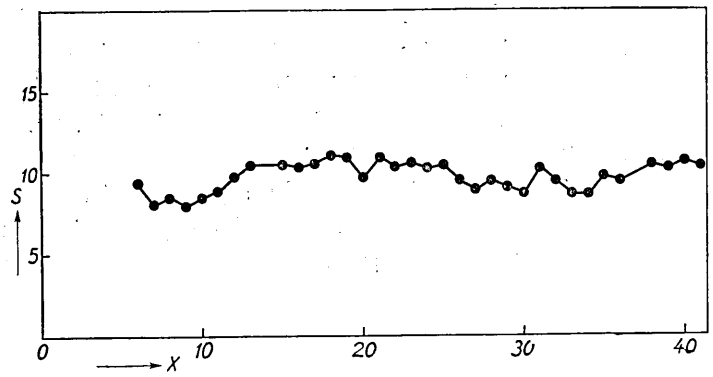

Fig. 69. Variation of S for Series VII.

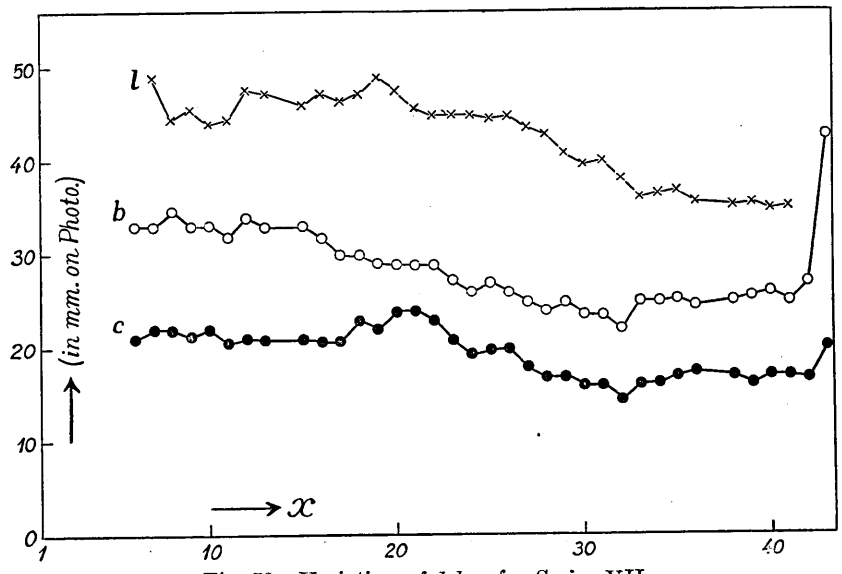

Fig. 70. Variation of l, b, c for Series VII.

the corresponding changes in S are not clearly apparent.

As to the lengths l, b, c, that is, BE, CF, CG, in Fig. 63, we cannot find any conspicuous changes corresponding to the changes in the stages as shown in Fig. 70, except that l and c decrease to a certain extent during the second stage, being approximately constant, in the third stage. At $x=43$, the amount of b is discontinuously increased which is the result of development of the second step of the slip lines.

5. Comparison with Results of Previous Experiments.

The mode of deformation of the sand mass in the present case is somewhat analogous to the deformation of the paraffin prism shown in

Nadai's book,[4] as regards the configuration of the slip lines developed. Fig. 20 shows a mode of deformation of the paraffin prism reproduced from Nadai's book. The main difference is in the boundary conditions. In the present case, the sand mass is piled in a vessel having glass lateral walls and a viscous substratum, whereas, in the case of the paraffin prism, the corresponding sides are all open.

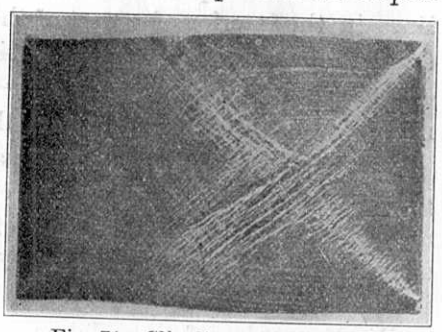

Fig. 71. Slip lines developed in paraffin prism. (Reproduced from Nadai's book)

On comparing the results of the present experiments with those of the previous ones in which the bed was rigid, we see several points of difference, which are evidently due to differences in the physical properties of the substratum.

i) As is apparent from the series of photographs, the configuration of the slip lines, that is, the slip planes, formed in the deformed sand mass is quite different, as illustrated schematically in Fig 72ab. This difference is evidently due to the presence of "Miduame" in the substratum, causing the sand mass to deform downward. Consequently, the development of the two systems of slip lines intersecting with each other at an angle $(\pi/2-\psi)$ initially becomes possible[5], and the slip lines which pass through the points B and E, in Figs. 59 and 72a, are actually developed.

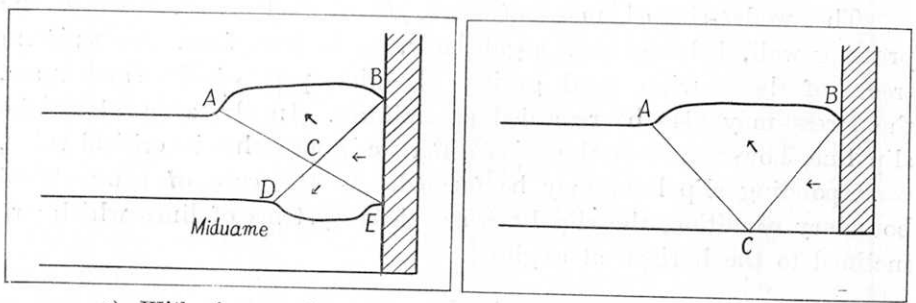

a) With viscous substratum. b) With rigid bed.

Fig. 72. Slip lines developed in the sand mass by lateral pressure.

4) NADAI, "Die plastische Zustand der Werkstoffe", (Berlin, 1927), 82.

5) For this, some discussions are given in the third report; T. TERADA and N. MIYABE, *loc. cit.* 1).

ii) In the experiments of Series VII, both the surface and the white lines in the interior of a part of the sand mass are tilted, when deformed, towards the direction of compression, while, in several of the previous experiments with rigid beds, they are tilted in the reversed sense. This may be connected with the fact that, in the present case, the traces of the moving sand grains in that part close to the slip line aA are sensibly greater than those in the part closer to the slip line ED, while, in several previous cases, the traces of the moving sand grains in the wedge-shaped part, EDB in Fig. 63a, of the sand mass were generally longer in the region closer to the front slip line farther away from the pressing wall. Examples of these latter cases are reproduced from the previous report in Fig. 73ab.

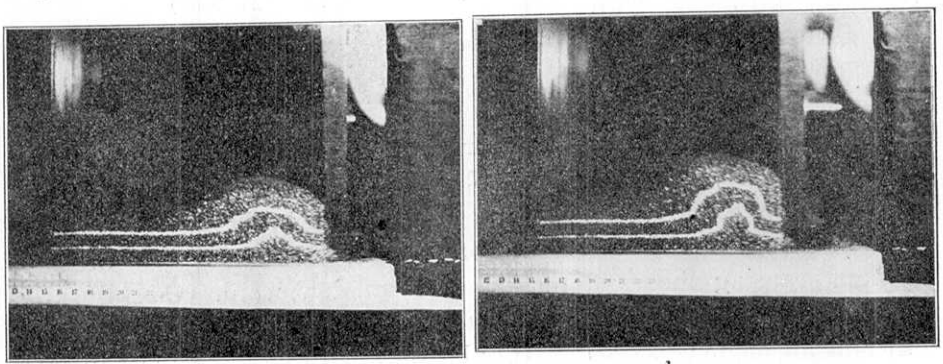

a b

Fig. 73. Tilting of the block of sand mass, when the bed is rigid.

The wedge-shaped mass of sand, BCF in Fig. 63, close to the pressing wall, behaves as a rigid body, as is seen from the uniform traces of the moving sand grains. In this part of the sand mass, the stress may also be regarded as uniform. In the zone along the slip line, however, since the stress difference approaches its critical value, corresponding slip lines may be formed. In the case of symmetrical boundary condition, the slip lines are those systems of lines which are inclined to the horizon at angles

$$\rho=\frac{\pi}{4}-\frac{\psi}{2}+\kappa,$$

and

$$\rho'=-\left(\frac{\pi}{4}-\frac{\psi}{2}\right)+\kappa,$$

as calculated for the case of passive pressure, by applying the theory of

earth pressure[6]. The angle κ in the above expression is the angle that the slip line makes with the axis of principal stress. Angle κ is also expressed as a function of two components of stresses σ_x, σ_y in the form

$$\sin 2\kappa=(\sigma_x-\sigma_y)/2K,$$

where K is the ultimate shear stress of the material for breaking. Another expression for κ has in the form

$$\tan\kappa=\frac{1}{\sqrt{n}},$$

where n is the axial ratio of the stress ellipses.

In the initial stage of deformation, the configuration of the slip lines formed in the sand mass seems to tend to be symmetrical in the upper and lower sides of the median line. But, as the deformation progresses, we observe, as a matter of fact, that the configuration of the slip lines becomes asymmetrical, consequently, angle ρ' is smaller in the lower part of the sand, from which it may be suggested that angle κ also is smaller due to the effect of the existing viscous substratum of "Miduame". The effect of the viscous substratum may be considered to be dependent on the rate of its deformation and the viscosity or plasticity of the material[7]. In the present case, however, the mode of deformation was affected not only by the mechanical properties of "Miduame" itself, but also by those of the surface crust that might have formed on the boundary of the sand and "Miduame". Thus, the viscous substratum appears to reduce the amount of angle ρ' or κ, as ψ is constant, that is, to reduce the stress difference $(\sigma_x-\sigma_y)$ or to magnify the axial ratio of the stress ellipse $n=\sigma_1/\sigma_2$. in the lower part of the overlying sand layer.

Correspondiug to such changes in the mechanical properties of the interior of the sand mass, we notice characteristic variations in the deviation in the height of CF in Fig. 59 (Series V) or CG in Fig. 63 (Series VII) from that of the median line, δH, in connection with the progress of the deformation. The variation in deviation, δH, for Series V and VII are plotted as usual against x, in Figs. 61 and 74.

In these curves, we notice that at the initial stage, the deviation δH tends to 0, which may be expected from the supposed configuration

6) KREY, "Erddruck, Erdwiderstand, *etc.*"

7) Considering a plastic material as loam or clay, the stress accumulated in it is shown to be a function of the rate of deformation or strain. c. f. S. KIENOW, *ZS. f. Geophys.*, 9 (1933), 204-229, etc.

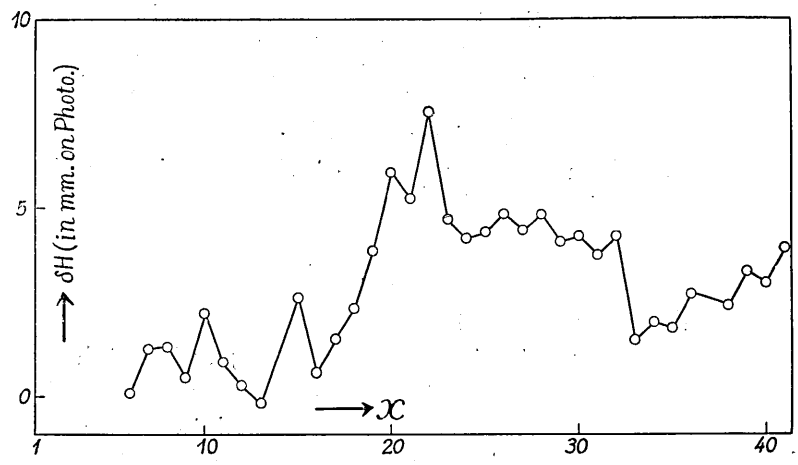

Fig. 74. The variation of δH, for Series VII.

of slip lines initially developed in the sand mass. In the curve of variation of δH for Series VII, conspicuous discontinuities are noticed at $x=22$ and $x=30$, corresponding to the discontinuities in the configuration of the slip lines, referred to above. It may also be worthy of notice that δH varies at the end of the first stage, similarly with the mode of variation of ζ. Since it is required geometrically that

$$\delta H=(\zeta+\zeta_0)\sin\theta',$$

the fact that the variation of δH is parallel with that of ζ shows that ζ_0 remains constant and the variation of $\sin\theta'$. i. e., from 0·5 to 0·7, is insignificant.

iii) The development of the step faults in the sand mass, as observed in the previous experiment with the rigid bed, may be expected to be difficult in the presence of a viscous substratum. As a matter of fact, step faults are not formed so frequently as in the experiments with rigid bed. Two factors may be considered to be related with this phenomenon. One of them is of course the presence of the viscous substratum, which will to some extent change the stress distribution in the interior of the sand mass, and the other the compactness of the sand mass connected with the velocity of the pressing wall.

A slow velocity of the pressing wall may have the same effect on the sand when it is loosely packed. In loosely packed sand, the slip lines formed by lateral pressure are not observed so clearly, but seem to be displaced gradually within a zonal region. The second slip line appears comparatively later than when the sand is closely packed, even if the

base is rigid. Since the bed in the present case, is of viscous it seems more difficult for the second slip line to develop.

As stated in the preceding reports, the configuration of the step faults and folds in the profiles of geological structure of several regions are found to be closely analogous to those of the slip lines developed in the sand mass upon being deformed by lateral pressure. Referring to the present experiment, it may be suggested that the step faults are formed in the superficial layers of the earth's crust of which the substratum does not behave as a viscous fluid, but rather as a rigid body.

6. Geophysical Applications. We find some geophysical phenomena analogous in their modes of deformation to those of the sand mass described in this paper.

In the Tango district, for example, block movements, as pointed out by Dr. C. Tsuboi[8], were a conspicuous feature of the earth's crust that occurred in association with the destructive earthquake of 1927. According to Tsuboi's investigations, the crustal blocks slipped up and down along the fault planes, in approximately the same way as traced by the geologists. A similar mode of block movements is also found in the crustal deformation in the Kwantô districts that occurred in association with the destructive earthquake of 1923[9]. In these actual cases, however, the earth's crust is assumed to consist of a number of crustal blocks bounded by geological faults, so that the mode of block movement may be restricted, geometrically, in which it differs from that of deformation of the sand mass.

A fact to which Dr. N. Nasu[10] has called attention is of interest here in connection with the present experiments. He projected the hypocentres of the after shocks that accompanied the Tango earthquake of 1927, on a plane perpendicular to the earth's surface and to one of the main faults, the Gô-mura Fault, and found that the origins of these after shocks are distributed on a system of planes inclined by several tens of degrees to the horizon. A similar distribution of origins of earthquakes is also observed in the Bôsô peninsula. The sensible earthquakes which occurred in the Bôsô peninsula[11] during 1924–1930, are distributed

8) C. Tsuboi, *Jap. Journ. Astr. Geophys.*, **11** (1933), 93-248.

9) N. Miyabe, *Bull. Earthq. Res. Inst.*, **9** (1931); **11** (1933), 639-692.

10) N. Nasu, *Journ. Fac. Sci.*, **3** (1929), 29-129.

11) The data of the epicentres and focal depths of these earthquakes are from the Seismometrical Report of the Institute, published in 1934.

horizontally as shown in Fig. 75, and the origins of these earthquakes being distributed vertically as shown projected on a vertical plane AB,

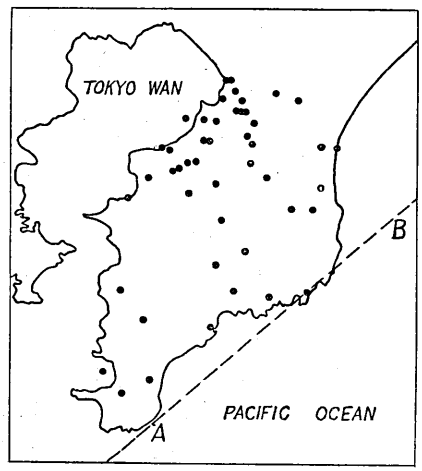

Fig. 75. Distribution of epicentres of the earthquakes in the Bôsô peninsula during 1924-1930.

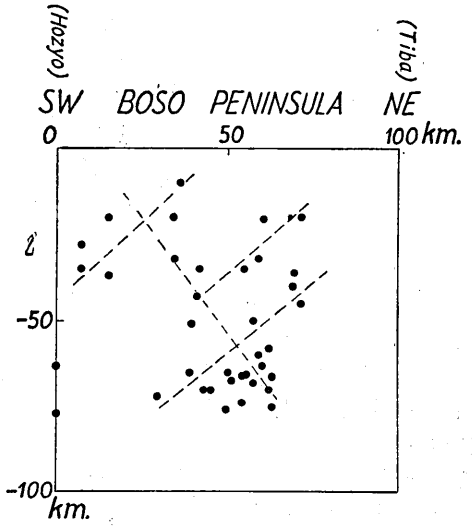

Fig. 76. Distribution of origins of earthquakes in the Bôsô peninsula as projected on a vertical plane parallel to the longer axis of the peninsula.

parallel to the longer axis of the peninsula. (See Fig. 76.) As may be suggested, the origins of these earthquakes are distributed approximately on planes inclined several tens of degrees to the horizon. The configuration of these planes may be noticed to be somewhat analogous to those of the slip planes, or lines, developed in the sand mass, on being subjected to lateral compression, although we do not know what really corresponds to the prime mover of our experiments in the formation of slip planes in the earth's crust.

7. Summary and Conclusion. In this paper, the writer has dealt with results of experiments on the deformation of a sand mass that is piled on a viscous substratum of "Miduame". The points in which the present experiments differ from the previous experiments with rigid bed are

i) The configuration of the slip lines or planes developed in the sand mass when it is exposed to lateral pressure;

ii) The sense of tilting, if tilted at all, of the block of the sand mass which is pushed upward;

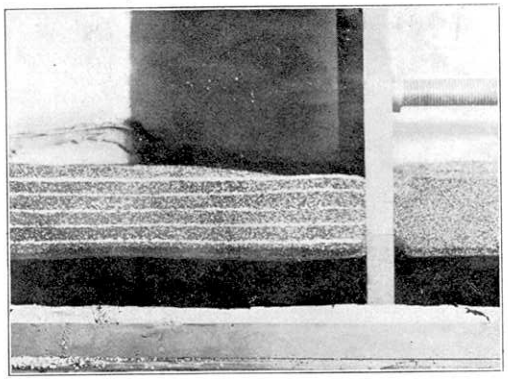

Fig. 11. $x=5$.

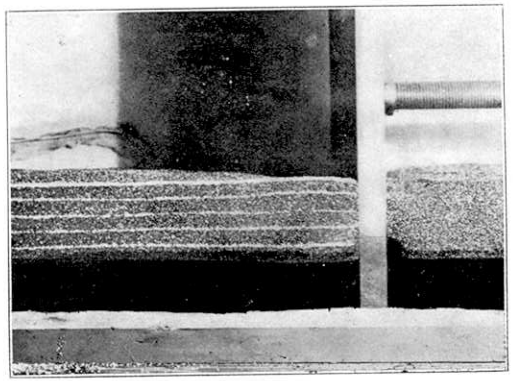

Fig. 12. $x=6$.

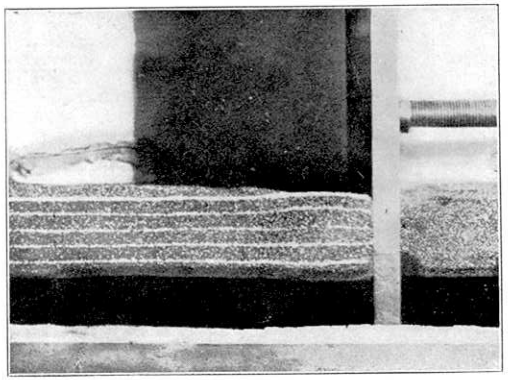

Fig. 13. $x=7$.

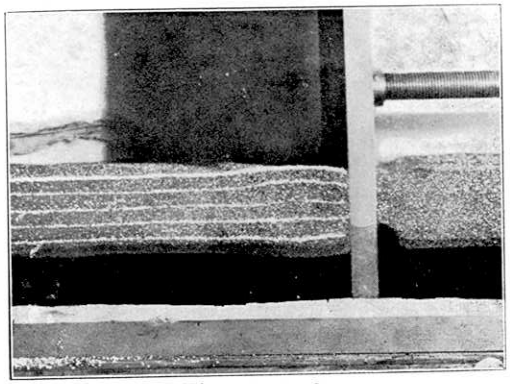

Fig. 14. $x=8$.

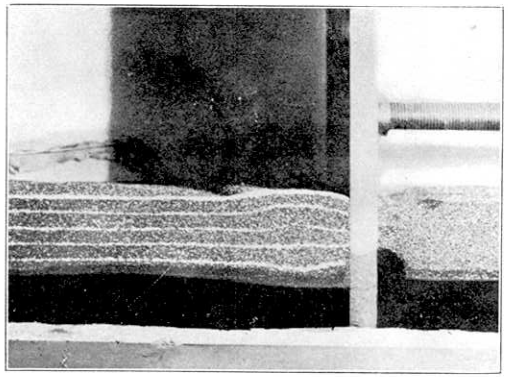

Fig. 15. $x=9$.

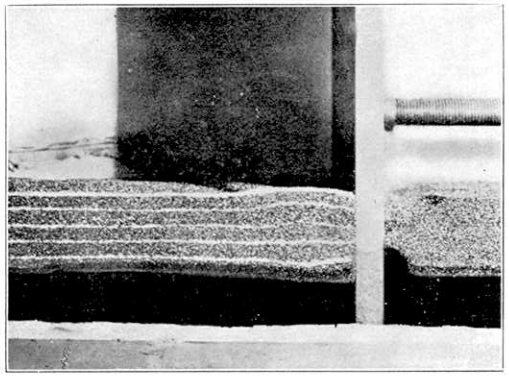

Fig. 16. $x=10$.

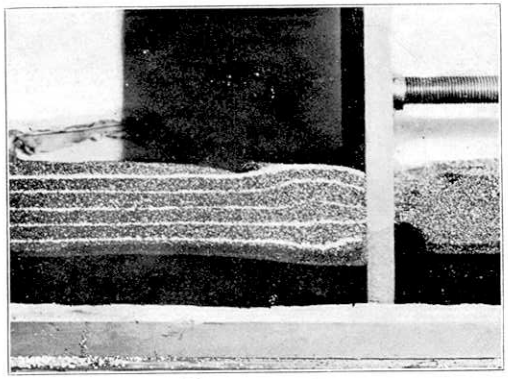

Fig. 17. $x=11$.

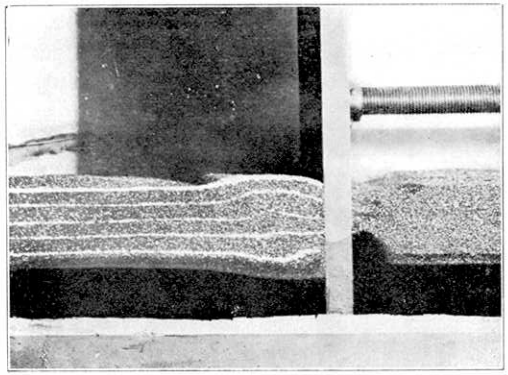

Fig. 18. $x=12$.

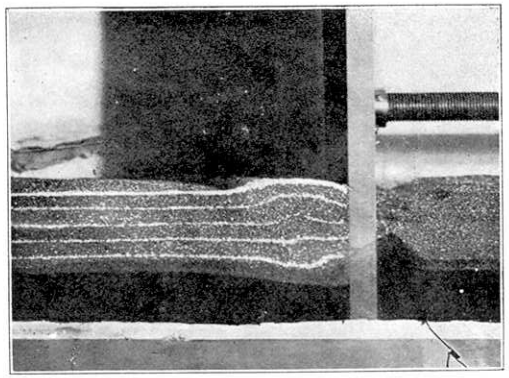

Fig. 19. $x=13$.

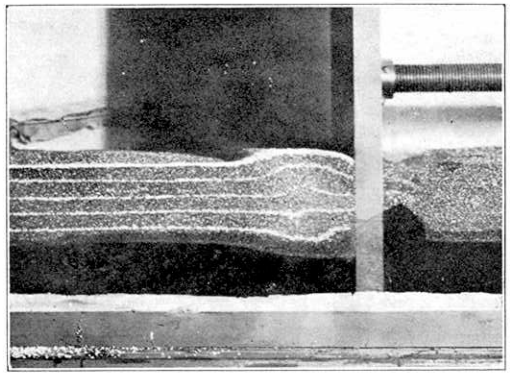

Fig. 20. $x=14$

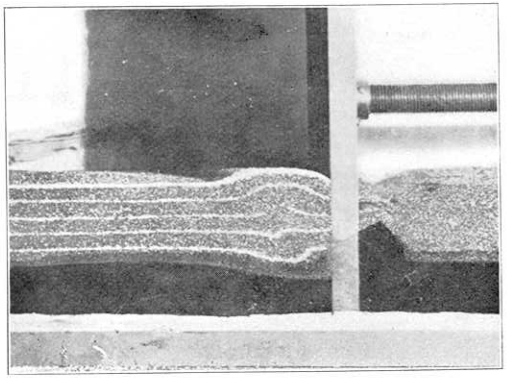

Fig. 21. $x=15$.

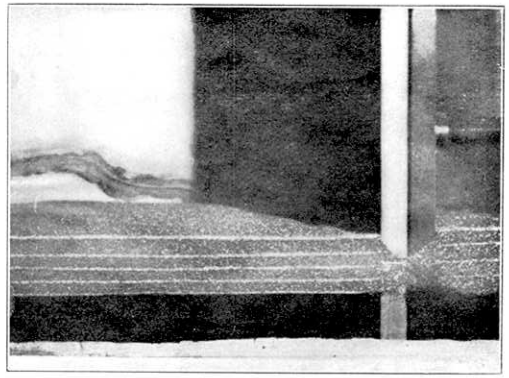

Fig. 22. $x=1$.

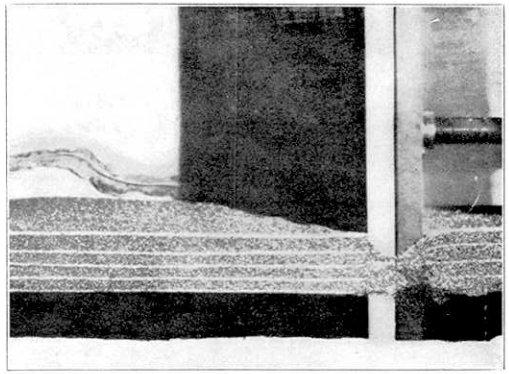

Fig. 23. $x=2$.

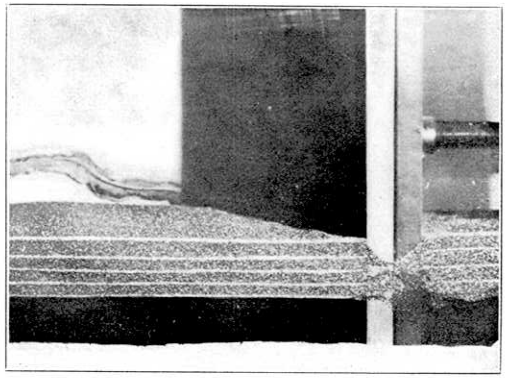

Fig. 24. $x=3$.

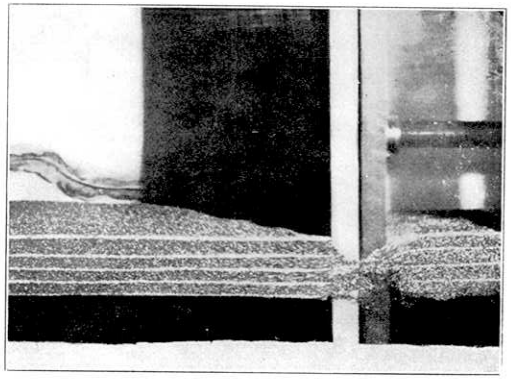

Fig. 25. $x=4$.

（震研彙報、第十二號、圖版、宮部）

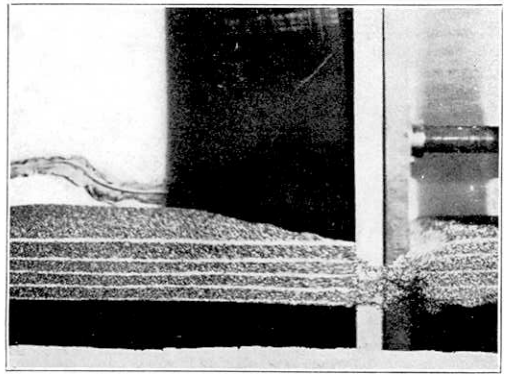

Fig. 26. $x=5$

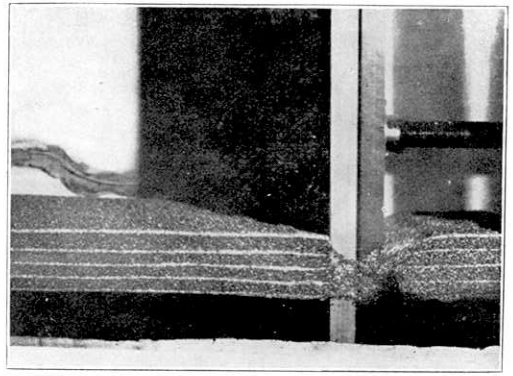

Fig. 27. $x=6$.

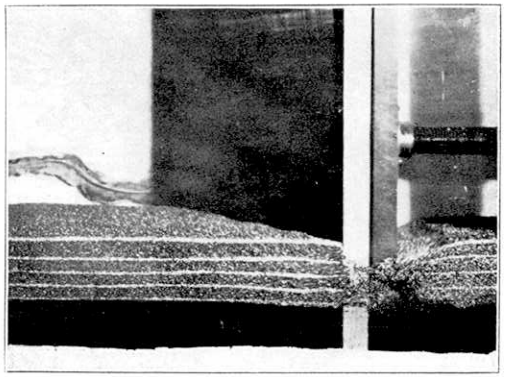

Fig. 28. $x=7$

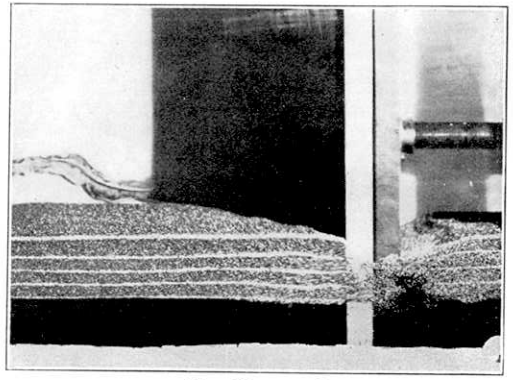

Fig. 29. $x=8$

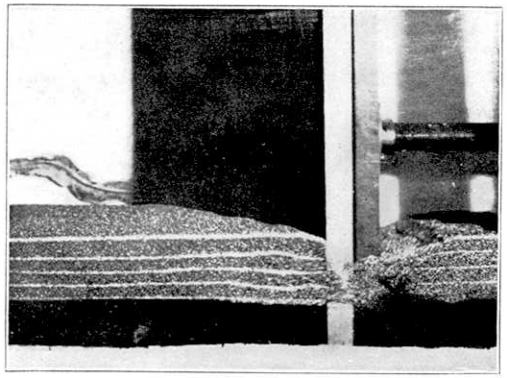

Fig. 30. $x=9$.

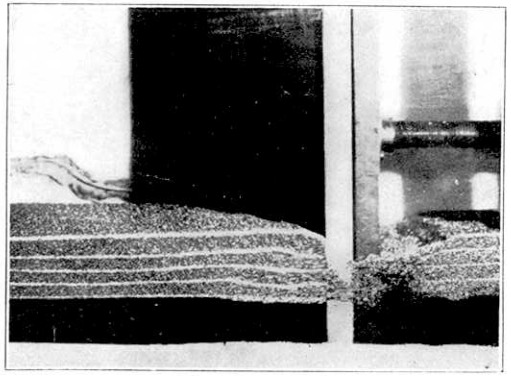

Fig. 31. $x=10$.

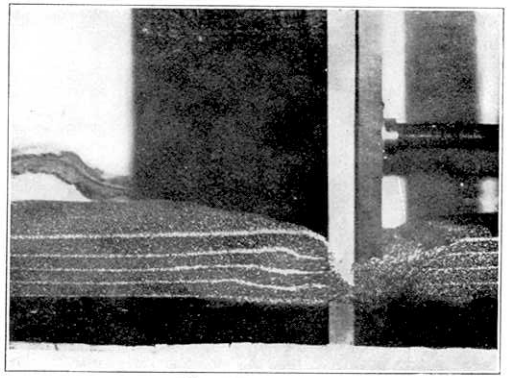

Fig. 32. $x=11$.

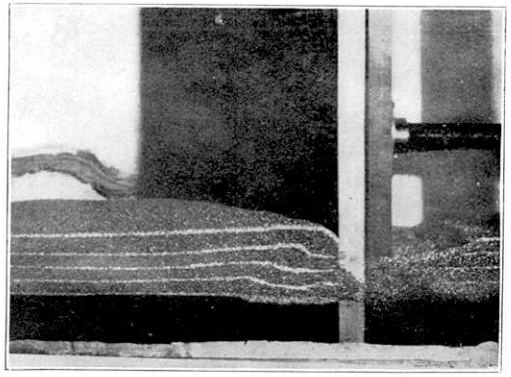

Fig. 33. $x=12$.

（震研彙報、第十二號、圖版、宮部）

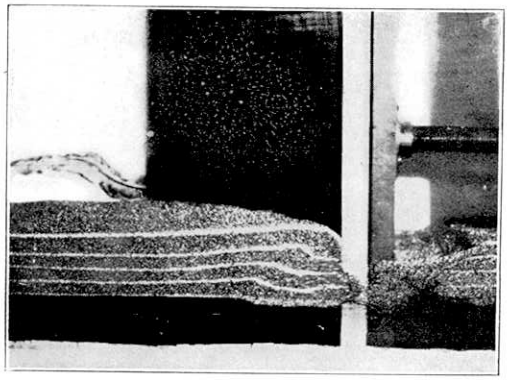

Fig. 34. $x=13$.

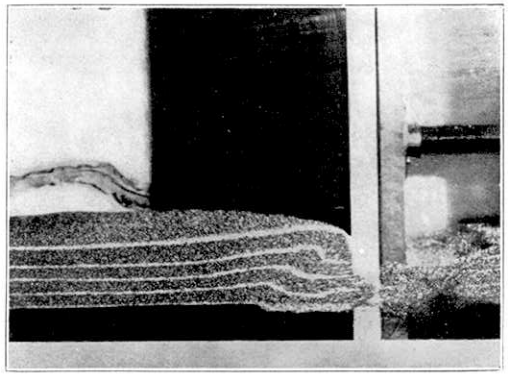

Fig. 35. $x=15$

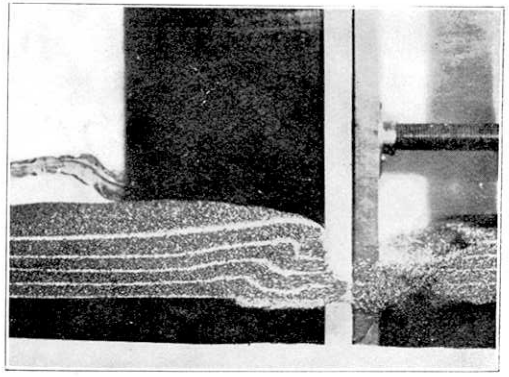

Fig. 36. $x=16$.

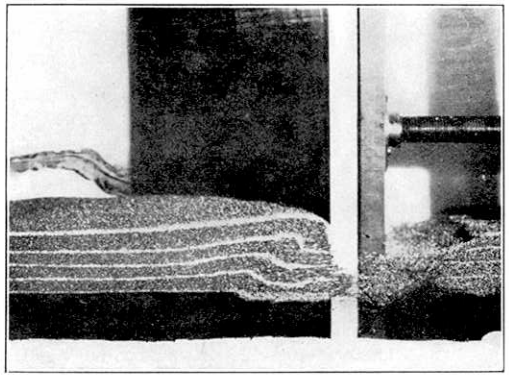

Fig. 37. $x=17$.

（震研彙報、第十二號、圖版、宮部）

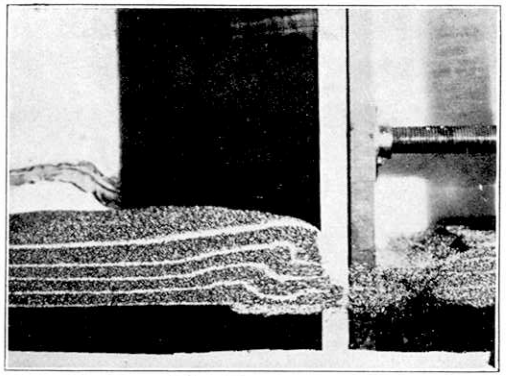

Fig. 38. $x=18$.

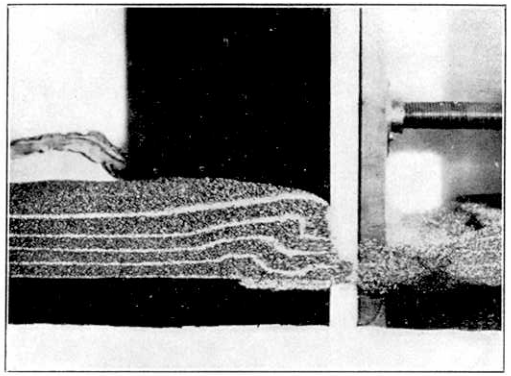

Fig. 39. $x=19$.

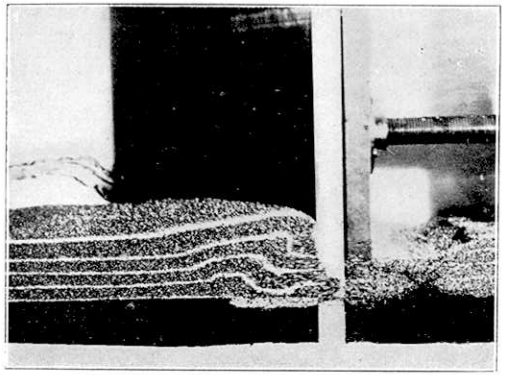

Fig. 40. $x=20$.

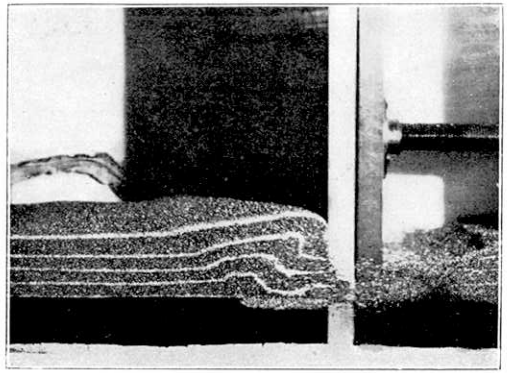

Fig. 41. $x=21$.

（震研彙報、第十二號、圖版、宮部）

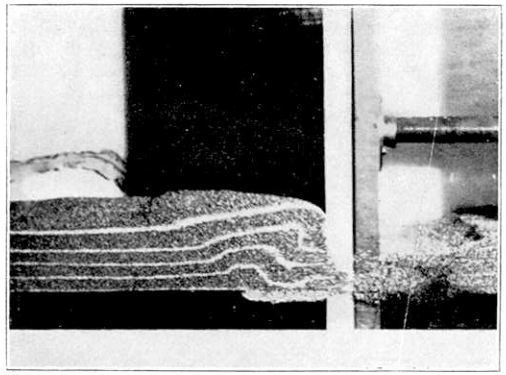

Fig. 42. $x=22$.

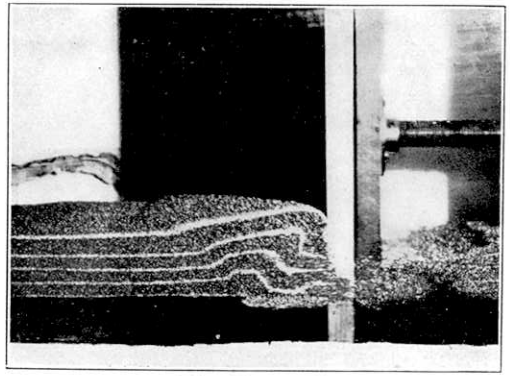

Fig. 43. $x=23$.

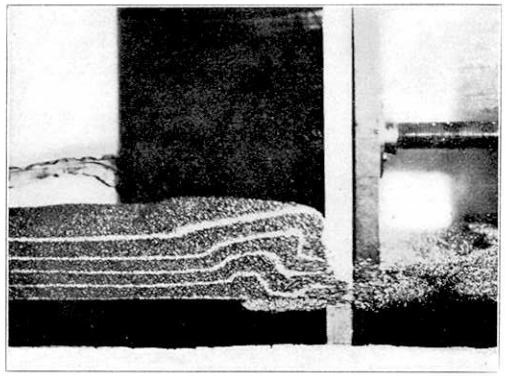

Fig. 44. $x=24$.

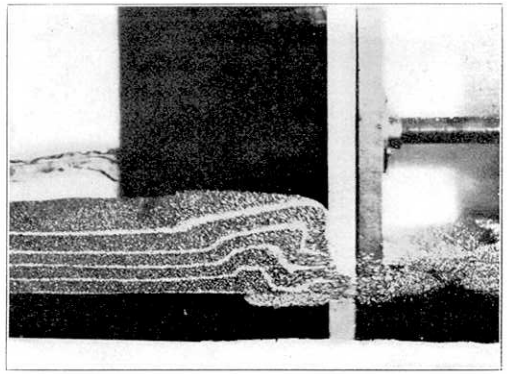

Fig. 45. $x=25$.

（震研彙報、第十二號、圖版、宮部）

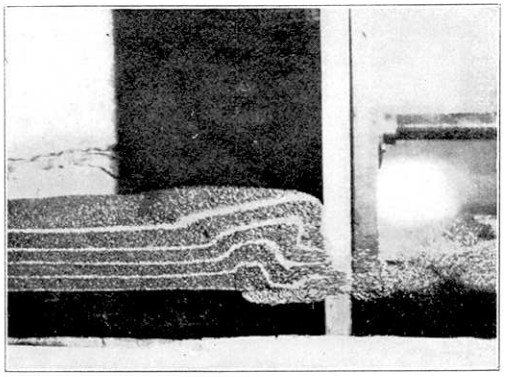

Fig. 46. $x=26$.

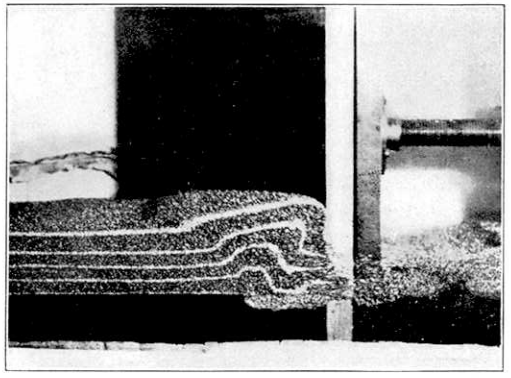

Fig. 47. $x=27$.

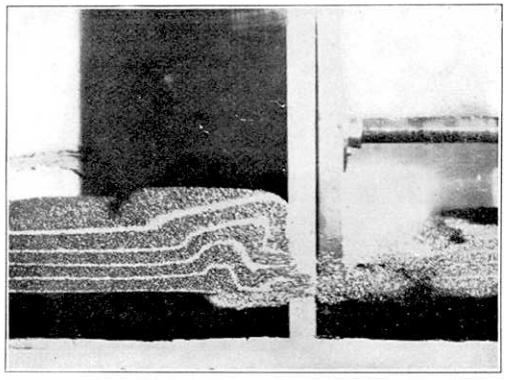

Fig. 48. $x=28$.

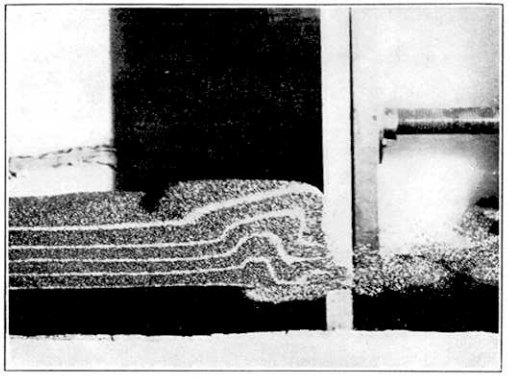

Fig. 49. $x=29$

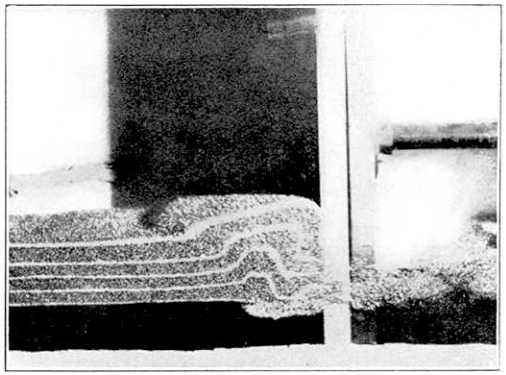

Fig. 50. $x=30$.

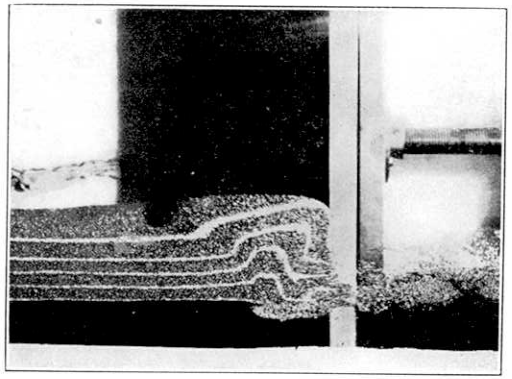

Fig. 51. $x=31$.

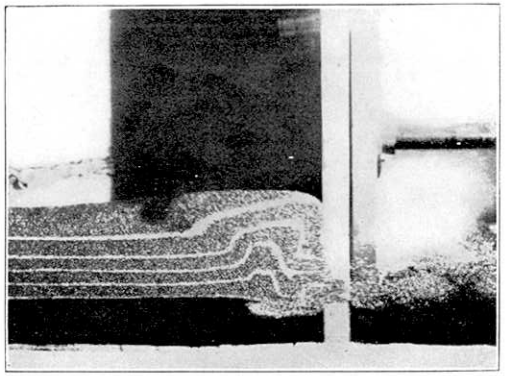

Fig. 52. $x=32$.

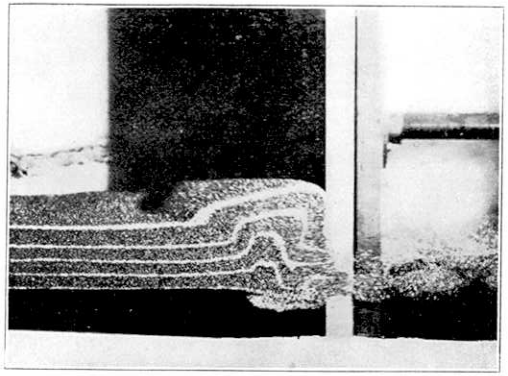

Fig. 53. $x=33$.

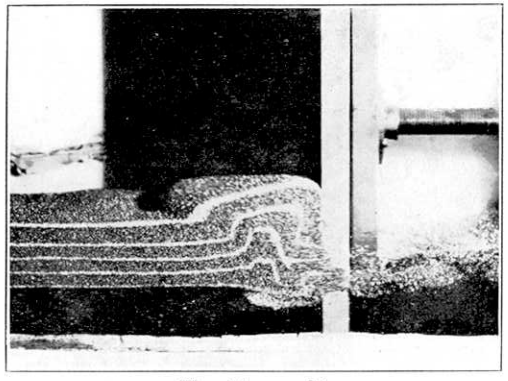

Fig. 54. $x=34$.

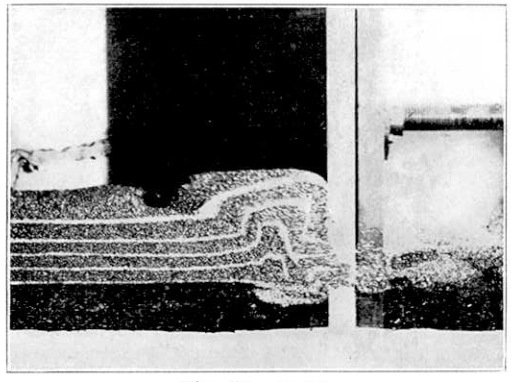

Fig. 55. $x=36$

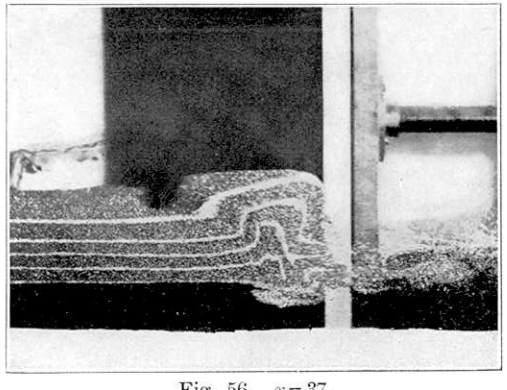

Fig. 56. $x=37$.

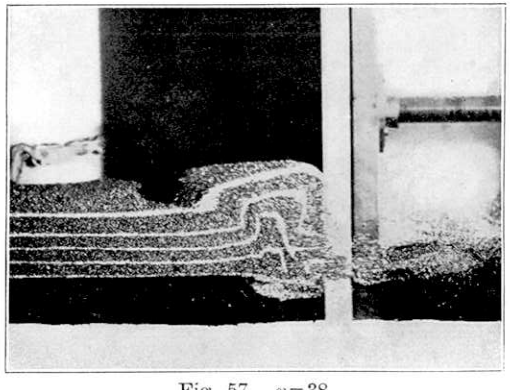

Fig. 57. $x=38$.

iii) The difficulty in the development of the second step of the slip line in the sand mass.

In the last paragraph are pointed out certain features of actual geophysical phenomena that are analogous to the results of the present experiments.

In conclusion, the writer wishes to express his sincere thanks to Professor Torahiko Terada, under whose guidance the present experiments were carried out.

---

14. 砂層の變形に關する實驗 (第 4 報)

地震研究所　宮　部　直　巳

砂層が水飴の層の上にある場合に横壓によつて如何に變形するかを調べた．第3報迄に就いて調べられた砂層の下底が剛體である場合に比較して異つた變形模様が見られる．下底が水飴であつて變形しやすい爲である．又水飴の表面に表皮の生ずることがあつて，その影響を受けることもある．

下底が剛體である場合の實驗の結果と比較して著しい差異は，

i) 砂層内に生ずる slip plane の様子が第 62 圖に比較されてゐるやうに全く異る．

ii) 變形する楔形の砂塊の傾動の起ることがあるが，下底が剛である場合と軟である場合(この實驗の場合) とではその向きが逆になる．

iii) 第2段の slip plane は現實驗の場合には生じ難い．尤もこれは，砂層の充塡狀態が粗である上に横壓の加へ方が甚だ緩である故にもよるかもしれないが，それのみによるものとは思はれない．

最後に，地質構造や地球物理學的現象の中の類例を擧げておいた．